Development 129, 2247-2258 (2002)
Printed in Great Britain © The Company of Biologists Limited 2002
DEV5007

Control of photoreceptor cell morphology, planar polarity and epithelial integrity during *Drosophila* eye development

Amanda T. Pickup[1], Michele L. Lamka[3], Qi Sun[4], Man Lun R. Yip[5] and Howard D. Lipshitz[1,2,*]

[1]Program in Developmental Biology, Research Institute, The Hospital for Sick Children, 555 University Avenue, Toronto, Ontario M5G 1X8, Canada
[2]Department of Molecular & Medical Genetics, University of Toronto, Toronto, Canada
[3]Department of Biology, University of Virginia, Charlottesville, VA 22904, USA
[4]Cornell Theory Center, Cornell University, Ithaca, NY 14853, USA
[5]OSI Pharmaceuticals, Uniondale, NY 11553, USA
*Author for correspondence (e-mail: lipshitz@sickkids.ca)

Accepted 4 February 2002

SUMMARY

We report that the *hindsight* (*hnt*) gene, which encodes a nuclear zinc-finger protein, regulates cell morphology, cell fate specification, planar cell polarity and epithelial integrity during *Drosophila* retinal development. In the third instar larval eye imaginal disc, HNT protein expression begins in the morphogenetic furrow and is refined to cells in the developing photoreceptor cell clusters just before their determination as neurons. In *hnt* mutant larval eye tissue, furrow markers persist abnormally posterior to the furrow, there is a delay in specification of preclusters as cells exit the furrow, there are morphological defects in the preclusters and recruitment of cells into specific R cell fates often does not occur. Additionally, genetically mosaic ommatidia with one or more *hnt* mutant outer photoreceptor cells, have planar polarity defects that include achirality, reversed chirality and misrotation. Mutants in the JNK pathway act as dominant suppressors of the *hnt* planar polarity phenotype, suggesting that HNT functions to downregulate JUN kinase (JNK) signaling during the establishment of ommatidial planar polarity. HNT expression continues in the photoreceptor cells of the pupal retina. When an ommatidium contains four or more *hnt* mutant photoreceptor cells, both genetically mutant and genetically wild-type photoreceptor cells fall out of the retinal epithelium, indicating a role for HNT in maintenance of epithelial integrity. In the late pupal stages, HNT regulates the morphogenesis of rhabdomeres within individual photoreceptor cells and the separation of the rhabdomeres of adjacent photoreceptor cells. Apical F-actin is depleted in *hnt* mutant photoreceptor cells before the observed defects in cellular morphogenesis and epithelial integrity. The analyses presented here, together with our previous studies in the embryonic amnioserosa and tracheal system, show that HNT has a general role in regulation of the F-actin-based cytoskeleton, JNK signaling, cell morphology and epithelial integrity during development.

Key words: *hindsight*, Eye, *Drosophila*, Planar polarity, Jun kinase, Epithelial integrity, F-actin, Morphogenesis

INTRODUCTION

Many developmental processes involve conversion of a monolayer epithelium into a differentiated tissue with numerous cell types and significant morphological complexity. As the epithelium differentiates, there are coordinated changes in cell fate, cell morphology, cell polarity and the relative positions of cells. The construction of a complex tissue from an undifferentiated epithelium is exemplified by the development of the *Drosophila* compound eye, which comprises an almost perfect array of roughly 750 unit simple eyes known as ommatidia (Wolff and Ready, 1993). Each ommatidium includes a central core of eight photoreceptor cells referred to as retinula or R cells (R1-6 are known as the 'outer' R cells while R7 and R8 are referred to as the 'central' R cells). The adult eye develops from an epithelial monolayer known as the imaginal eye disc. The R cell precursors are first specified in the late third instar larval disc, when a dorsoventral groove, called the morphogenetic furrow, sweeps across the disc from the posterior to the anterior and leaves organized clusters of R precursor cells in its wake (Ready et al., 1976; Tomlinson, 1985; Tomlinson and Ready, 1987). During larval and pupal stages, a plethora of gene products regulate cell division, cell specification, relative cell shape and movement, as well as programmed cell death in the developing retina (Cagan and Ready, 1989a; Wolff and Ready, 1991).

One of the developmental events initiated shortly after specification of clusters of presumptive R cells is establishment of planar polarity in the imaginal disc epithelium. In a process regulated by so-called 'tissue polarity' genes, each of the R-cell precursor clusters senses the direction of the furrow progression and receives polarity information from its more

mature neighbors (reviewed by Mlodzik, 1999). The R-cell cluster rotates through 90°, so that the R3/R4 pair, which initially faced the furrow, comes to face the dorsal or ventral pole of the disc. This rotation occurs in opposite directions in the dorsal and ventral halves of the disc, creating an axis of global mirror image symmetry known as the equator. Each cluster also loses its initial bilateral symmetry and becomes chiral as the R4 cell loses contact with the R8 cell and moves to a more equatorial position. The Jun kinase (JNK) signaling pathway has been shown to play a prominent role in creating the distinction between R3 and R4 cell fates during the establishment of planar polarity in the eye (Weber et al., 2000). When an activated form of the JUN transcription factor is expressed in the R3 and R4 precursor cells, it gives rise to a symmetrical, a misrotated or a chirally reversed ommatidium (Weber et al., 2000).

During pupal stages, the apical faces of the R cells undergo a stereotypical series of interactions that are associated with the expansion of the apical surface downwards to meet the cone cell plate at the floor of the ommatidium (Longley and Ready, 1995; Sang and Ready, 2002). The apical surface of each R cell is mechanically anchored to the cone cell plate prior to further deepening of the retina (Cagan and Ready, 1989a; Longley and Ready, 1995). As terminal differentiation occurs, a photosensitive organelle – the rhabdomere – forms at the apical surface of each R cell and eventually spreads down the entire cell length. The apical faces of the interacting R cells, which are enriched for F-actin, Armadillo, DE-cadherin and Crumbs, are dynamically rearranged during photoreceptor morphogenesis (Sang and Ready, 2002). It is not clearly understood what molecules direct the longitudinal expansion of the apical surface or of its rhabdomere, although recent evidence suggests a role for *eyes closed*, which encodes the p47 co-factor of a p97 ATPase that is implicated in membrane fusion, in regulation of photoreceptor morphogenesis (Sang and Ready, 2002).

The *hindsight* (*hnt*) gene (*peb* – FlyBase) encodes a nuclear zinc-finger protein with all of the hallmarks of a transcription factor (Yip et al., 1997). In the embryo, *hnt* function is required for germband retraction (Lamka and Lipshitz, 1999; Yip et al., 1997), dorsal closure (Reed et al., 2001) and tracheal morphogenesis (Wilk et al., 2000). Expression of the *hnt* gene is required in the amnioserosa to downregulate JNK signaling in that tissue and to create a sharp distinction between the epidermal and amnioserosal tissue (Reed et al., 2001). In *hnt* mutants, the expression of the JUN target genes, *decapentaplegic* (*dpp*) and *puckered* (*puc*), persists inappropriately in the amnioserosa, leading to failure of dorsal closure (Reed et al., 2001). The leading edge cells of the epidermis neither undergo appropriate cell shape changes nor accumulate apicolateral F-actin or phosphotyrosine-containing proteins characteristic of the focal complex seen in wild-type embryos at the boundary between the leading edge and the amnioserosa (Reed et al., 2001). In addition to a role in regulating JNK signaling during dorsal closure, HNT function is necessary for the maintenance of tracheal epithelia (Wilk et al., 2000). In *hnt* mutants the tracheal system initially develops normally but, by stage 15, the epithelium loses its integrity and forms sacs and vesicles. The mutants also lack apical extracellular structures known as taenidia, suggesting that terminal differentiation of the tracheal cells is defective (Wilk et al., 2000).

We describe the role of HNT during eye development. We show that the HNT protein is expressed in all of the photoreceptor cell precursors in developing eye discs. Examination of a *hnt* temperature-sensitive allele and analyses of chimeras carrying patches of cells homozygous for lethal *hnt* alleles suggest that there are at least five functions of HNT during eye development. First, HNT is necessary immediately posterior to the morphogenetic furrow for the correct morphology and arrangement of cells in the ommatidial precluster (which contains the R8, R2, R5, R3 and R4 precursor cells), as well as for the specification of the R2, R5, R3 and R4 precursor cells. Second, HNT function is necessary in the outer R cells for the establishment of correct chirality and rotation of the ommatidia. This tissue polarity function may involve downregulation of the JNK signaling cascade by HNT. Third, HNT function is required to maintain ommatidial structure and integrity during the mid-pupal stage. Fourth, HNT function is required in each R cell to accomplish apical-basal extension of the cell and its rhabdomere as the adult retina is assembled in the pupal period. Finally, HNT function is required for the separation of the rhabdomeres of neighboring cells that occurs during the late pupal period. Thus, HNT possesses both eye-specific functions (precluster patterning) and general functions (regulation of the F-actin-based cytoskeleton, regulation of JNK-mediated processes, control of tissue integrity) in development. We speculate that regulation of a single molecular pathway involving cell-cell or cell-extracellular matrix adhesion, or communication, underlies all of these functions.

MATERIALS AND METHODS

Drosophila mutants and lines

The following fly stocks were used in this study: hnt^{XO01}, hnt^{EH704a}, hnt^{XE81}, hnt^{peb} (Yip et al., 1997), hnt^{1142} (Wilk et al., 2000), jun^{1} (Kockel et al., 1997), $jun^{76–19}$ (Hou et al., 1997), bsk^{1} and bsk^{2} (Sluss et al., 1996), rho^{PX81} (Freeman et al., 1992), *dpp-lacZ* BS3.0 (Blackman et al., 1991), and N^{ts1} (Cagan and Ready, 1989b; Shellenbarger and Mohler, 1975). The FRT line w^{1118} *P{w*$^{+mC}$*=piM}5A P{w*$^{+mC}$*=piM}10D P{ry*$^{+t7.2}$*=neoFRT}18A* and the FLP recombinase stock w^{1118}*; MKRS, P{ry*$^{+t7.2}$*=hsFLP}86E/TM6B,* Tb^{1} were obtained from the Bloomington *Drosophila* Stock Center.

FLP-induced clones in the eye disc

Clones were induced in the eye according to standard protocols (Harrison and Perrimon, 1993; Xu and Rubin, 1993). First instar larvae were heat-shocked for 1.5 hours in a waterbath at 38.5°C. Larval eye discs were dissected from third instar larvae and double antibody stained with the antibody of interest and α-HNT, the latter enabling identification of clones. Scars were scored in the adult or pupa and these were found at a frequency of approximately 50% among the class of flies that had the genotype required for a FLP-induced event.

Immunohistochemistry, histochemistry, X-Gal staining, histology and microscopy

Antibody staining of eye discs was carried out using standard protocols (Wolff, 2000). Primary antibodies used were: mouse α-HNT monoclonal (27B8 1G9 at 1:25 dilution) (Yip et al., 1997); rabbit α-β-Galactosidase (α-β-gal; 1:1000; Cappel); mouse α-Phosphotyrosine monoclonal (α-PY; 1:500, Upstate Biotechnology), mouse α-Boss monoclonal (at 1:1000 dilution) (Van Vactor et al., 1991); rabbit α-Spalt (at 1:500 dilution) (Barrio et al., 1999), mouse α-Glass

monoclonal (at 1:5 dilution) (Moses and Rubin, 1991). All secondary antibodies were used at a dilution of 1:250 and were obtained from Jackson Immunoresearch: these were horseradish peroxidase (HRP) conjugated goat α-mouse antibody, HRP-conjugated goat α-rabbit antibody, FITC-conjugated goat α-mouse antibody and TRITC-conjugated goat α-mouse antibody. Visualization of F-actin using FITC-conjugated phalloidin (Sigma) was according to Wolff (Wolff, 2000). X-Gal staining was carried out as described elsewhere (Wolff, 2000). For double staining with the α-HNT antibody, the discs were first fixed in 4% formaldehyde in 1×phosphate-buffered saline (PBS) on ice. The X-Gal staining was then carried out overnight. Afterwards, the discs were washed thoroughly and then placed in primary α-HNT antibody. The rest of the protocol was carried out as for antibody staining. Cell death was detected using an Apoptag S1760 direct detection kit (Intergen). Standard methods were used to prepare histological sections of adult eyes (Tomlinson and Ready, 1987). A Zeiss Axioplan microscope was used for light microscopy and images were captured with a Spot digital camera (Diagnostic Instruments). A Zeiss Axiovert 100 microscope with LSM510 software was used for laser confocal microscopy. Images were processed and displayed using Photoshop software (Adobe). Samples were prepared for scanning electron microscopy (SEM) using standard methods (Ready et al., 1976). A Hitachi S570 microscope was used to view the eyes.

Heat treatments

For the *Notch* experiment, N^{ts1} larvae were shifted to 32°C for 24 hours as described elsewhere (Cagan and Ready, 1989b). Third instar larval discs were then dissected and stained with the α-HNT antibody. For temperature shift experiments, 1 hour hnt^{peb} egg collections were raised at either 18°C or 29°C and then shifted either up or down at 12 hour intervals. Once adult flies had eclosed, their eyes were scored for external roughness under a dissecting microscope.

RESULTS

Hindsight protein is expressed in neuronal precursor cells in the larval eye imaginal disc

To study Hindsight (HNT) protein expression we used a mouse monoclonal antibody (α-HNT) that specifically recognizes the HNT gene product as it does not stain *hindsight* (*hnt*) mutant embryos (Yip et al., 1997). In the third instar larval eye disc (Fig. 1A), HNT first accumulates in cells in the middle of the furrow partially overlapping with *decapentaplegic* (*dpp*) reporter gene expression (Fig. 1B). The most anterior edge of HNT expression appears serrated (Fig. 1C). In the posterior part of the furrow, HNT expression is found in all cells. Posterior to the furrow, HNT expression resolves to only the photoreceptor (R) cell precursors (Fig. 1D). This refinement most probably reflects a negative regulation of HNT expression in non-neuronal precursor cells behind the furrow and is consistent with HNT expression being a read-out of neuronal fate. The pattern of HNT staining in the R cell precursors prefigures the sequence of their neuronal determination (i.e. R8, R2, R5, R3 and R4 stain by row two, R1 and R6 stain by row four, and R7 stains by row six). From rows two to six, HNT expression is slightly higher in the R3 and R4 precursor cells relative to the rest of the cells within the clusters (Fig. 1D inset). This is the stage at which the R3 and R4 cells sense the signals that determine ommatidial planar polarity. HNT is also expressed in the ocellar precursor cells found in the anterior portion of the eye disc (Fig. 1A) but is not found in the cone or pigment cell precursors in either larval or pupal discs. HNT is, however, expressed in the bristle cell precursors in pupal eye discs (Fig. 1E).

HNT is also present in sensory neuron precursor cells in all other discs, including the wing disc (Fig. 1F), the leg disc (Fig. 1G) and the antennal region of the eye-antennal disc (Fig. 1A). The identity of these HNT-positive cells was confirmed by double antibody staining discs from A101 larvae, which have an enhancer trap in the *neuralized* gene (Boulianne et al., 1991; Huang et al., 1991), where there is β-gal expression in all sensory neuron precursor cells (data not shown).

In a $Notch^{ts1}$ mutant in which the function of the NOTCH receptor has been reduced, neural hypertrophy occurs in the discs (Cagan and Ready, 1989b). In $Notch^{ts1}$ discs, HNT protein is expressed in the supernumerary neuronal precursor cells (compare Fig. 1G with 1H). Thus, HNT expression in neuronal precursor cells is a read-out of sensory neuron specification. This experiment also demonstrates that wild-type Notch function is not required for HNT expression.

HNT is required for R cell fate specification and ommatidial cluster morphogenesis

To understand the role of HNT during eye development, we undertook a phenotypic analysis of the viable $hnt^{pebbled}$ (hnt^{peb}) mutant, which has a temperature-sensitive rough eye phenotype (Fig. 2) (Yip et al., 1997). In addition, we analyzed three lethal, antibody-null alleles of *hnt*: hnt^{XE81} and hnt^{EH704a}, which behave as genetic nulls, and hnt^{XO01}, which behaves as a strong hypomorph (Yip et al., 1997). The lethal *hnt* mutations fail to complement the hnt^{peb} rough eye phenotype (Fig. 2C) (Yip et al., 1997). To examine the consequences of removing HNT function in the eye disc we generated patches ('clones') of cells homozygous for the lethal *hnt* alleles using the FLP/FRT recombination system (Golic, 1991).

In wild type, the *dpp-lacZ* reporter gene marks all cells in the furrow and is abruptly downregulated in the preclusters as they emerge posterior to the furrow (Fig. 3A) (Blackman et al., 1991). In patches mutant for the hnt^{XE81} allele, the expression of the *dpp-lacZ* gene is normal (Fig. 3B). However, in hnt^{peb} (Fig. 3C) and in patches mutant for the hnt^{XO01} hypomorphic allele (Fig. 3D), *dpp-lacZ* expression is normal in the furrow but persists posterior to the furrow in some R cells. The effect was more severe in the hnt^{peb} mutant than in hnt^{XO01} patches. These results support a role for HNT in downregulating *dpp* posterior to the furrow. The absence of an effect in strong *hnt* mutants (i.e. hnt^{XE81} and hnt^{EH704a}) suggests that there may be a positive feedback loop between DPP signaling and HNT; thus, the effect is only revealed when there is some residual HNT function.

Staining of hnt^{peb} discs and *hnt* patches with markers for neuronal determination showed that there is a delay in R-cell precluster formation posterior to the furrow in *hnt* mutants. For example, in *hnt* patches there is a one- to two-row delay (representing 2-4 hours) in expression of the marker recognized by α-HRP (Fig. 3E) and of Elav (data not shown) relative to the adjacent wild-type region of the epithelium.

We next examined early cluster morphology using the α-phosphotyrosine antibody (α-PY) that highlights all cell membranes, particularly those of the R cells (Fig. 3F). The α-PY antibody outlines the arc stages in row one at the posterior edge of the furrow [the normal developmental progression in cluster morphology is reviewed by Wolff and Ready (Wolff and

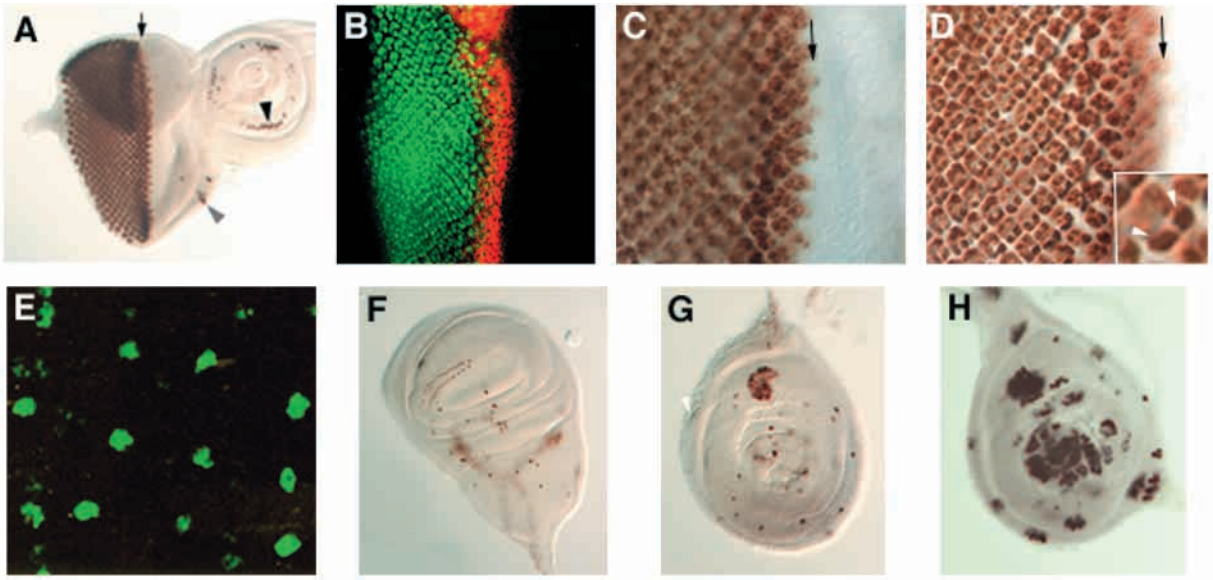

Fig. 1. HNT is expressed in sensory neuron precursor cells in larval discs. Third instar larval and pupal discs stained with α-HNT antibody: (A-D) larval eye discs; (E) pupal eye disc; (F) wing disc; (G,H) leg discs. (A) In wild type, HNT accumulates posterior to the morphogenetic furrow of the eye disc (arrow) in the nuclei of all R cells before their differentiation as neurons, in all sensory neuron precursor cells in the antennal disc (black arrowhead points to a subset of these cells) and in the ocellar precursor cells (gray arrowhead). (B) Eye disc from a larva carrying a *dpp-lacZ* enhancer trap (see Materials and Methods) double-stained with α-HNT antibody (green) and an α-β-gal antibody to visualize *dpp*-reporter expression (red). The most anterior boundary of HNT expression is in the middle of the furrow, partially overlapping with *dpp*-reporter expression. (C) HNT expression in the furrow is restricted to clusters of cells, with non-staining cells in between (the arrow marks the furrow). (D) More posteriorly, HNT is found in the nuclei of all R cells in the developing clusters (the arrow marks the furrow). Inset: there is higher accumulation of HNT in the R3 and R4 precursor cells (white arrowheads). (E) HNT accumulates in the bristle precursor cell nuclei in the basal plane of a pupal eye disc. (F,G) HNT accumulates in sensory precursor cells in third instar wing (F) and leg (G) discs. (H) In a leg disc from a N^{ts1}/Y fly pulsed at the restrictive temperature, HNT accumulates in the additional cells that are now destined to become neurons.

Ready, 1991)]. In *hnt* mutant patches the arcs appear to form normally and at evenly spaced intervals (Fig. 3F). Within the *hnt* mutant tissue, the earliest defects involve cluster shape and cell number at the five cell precluster stage (Fig. 3F). In mutant patches, the definitive preclusters usually have the normal number of cells (five; R8, R2, R5, R3, R4) but, occasionally (i.e. in fewer than 5% of the preclusters), there are missing cells or additional cells with high levels of α-PY staining. More strikingly, some of the preclusters either have cells misarranged relative to one another or the cluster does not rotate properly.

Glass is normally expressed in all presumptive R cells (Moses and Rubin, 1991). In eye discs from hnt^{peb} larvae, most precluster cells express Glass (compare Fig. 3G with 3H), indicating they have attained a photoreceptor identity. However (Fig. 3H), some of these preclusters are missing Glass-positive cells (22%, *n*=46), have displaced cells (30%, *n*=46) or have additional posterior cells (17%, *n*=46). The frequency of these defects in Glass staining is five- to tenfold higher than the frequency of preclusters with missing or additional cells as assayed using α-PY. A likely explanation for this difference in frequencies is that the correct number of cells is recruited into definitive preclusters in *hnt* mutants but that these cells have a reduced ability to achieve presumptive R cell fate.

To examine whether specification of individual R cell fates proceeds normally in *hnt* mutants, we used three markers that label the early R cells. These are the α-Boss antibody, which labels determined R8 cells beginning three rows posterior to the furrow (Van Vactor et al., 1991); the *rhomboid* enhancer trap, rho^{PX81}, which is expressed strongly in R8, R2 and R5, beginning two rows posterior to the furrow (Freeman et al., 1992); and the α-Spalt antibody, which

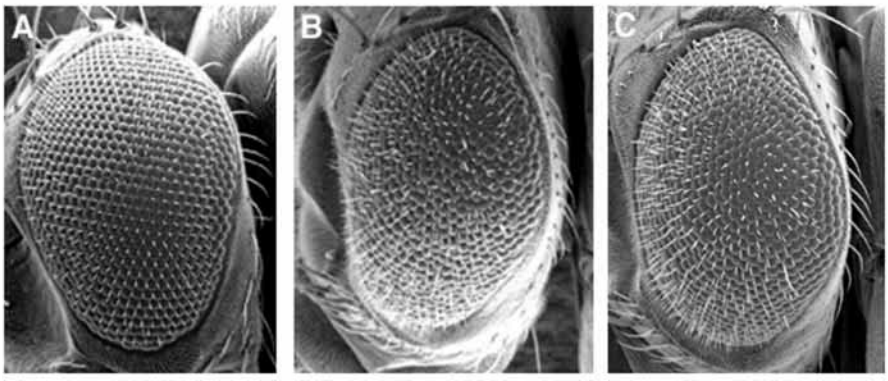

Fig. 2. hnt^{peb} is a viable allele that causes eye roughening. Scanning electron micrographs of adult eyes. (A) Wild-type eye. Note the regular arrangement of facets. (B) Eye from a hnt^{peb}/hnt^{peb} fly raised at the restrictive temperature. Note the disorganized facets, causing roughening. (C) Eye from a hnt^{peb}/hnt^{XE81} fly. Note the similar phenotype to that shown in B. This failure to complement hnt^{peb} was observed for three other alleles of *hnt* (hnt^{EH704a}, hnt^{XO01} and hnt^{1142}; data not shown). In all cases, anterior is towards the left and dorsal is towards the top of the page.

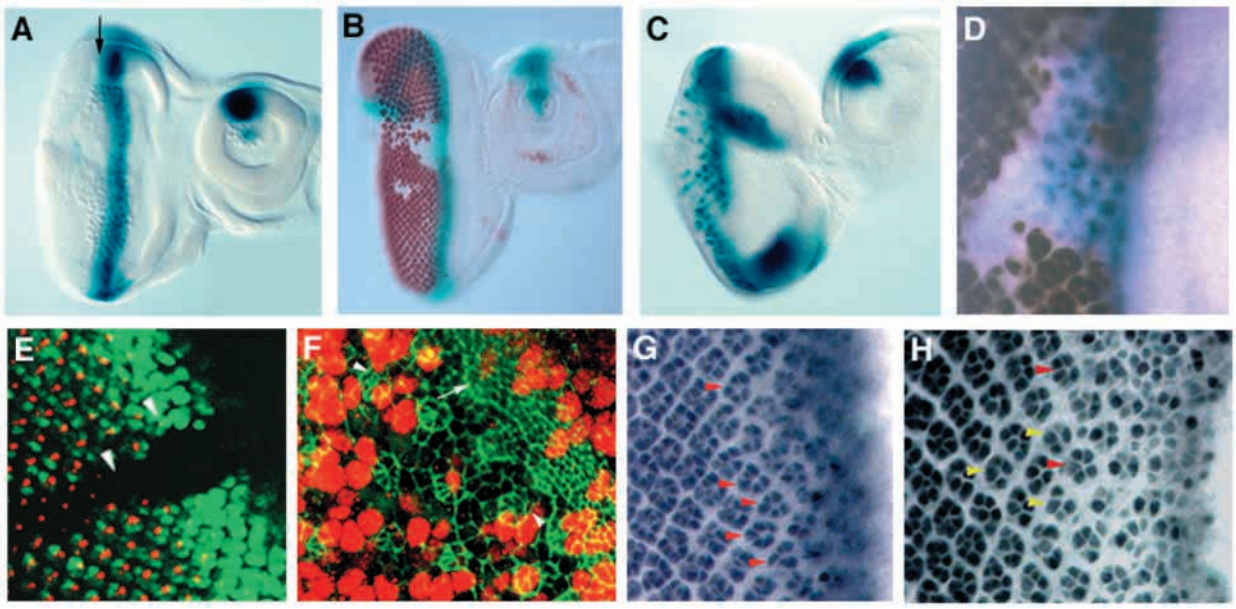

Fig. 3. *dpp* expression, neuronal determination and precluster formation in *hnt* mutant eye discs. (A-D) Expression of a *dpp-lacZ* reporter in wild-type (A) and *hnt* mutant (B-D) eye tissue. (A) In a late third instar disc from a *dpp-lacZ*/+ larva, reporter expression occurs along the furrow and is abruptly downregulated posterior to the furrow. The arrow marks the posterior border of the furrow. The reporter was visualized by X-Gal staining. (B) A disc with a hnt^{XE81} clone visualized by the lack of α-HNT antibody staining (brown) behind the furrow. The *dpp-lacZ* reporter expression, visualized by X-Gal staining, looks normal. The same result was obtained with hnt^{EH704a} clones (not shown). (C) A disc from a hnt^{peb}/Y larva raised at the restrictive temperature, showing that the *dpp*-reporter expression is no longer tightly downregulated at the posterior edge of the furrow but persists in some of the emerging clusters in the eye field (reporter was visualized by X-Gal staining). (D) A disc with a hnt^{XO01} clone, showing that the *dpp*-reporter expression (blue-black staining), again persists posterior to the furrow, when it would normally be shut off. In this case, reporter expression was visualized with α-β-gal antibody. (E) Eye disc containing a hnt^{XE81} clone visualized by lack of immunostaining with α-HNT antibody (HNT-expressing cells are green). α-HRP staining (red) labels clusters of neuronally determined R cell precursors. Within the *hnt* tissue, the neuronal determination in the clusters is delayed relative to the adjacent wild-type clusters. The white arrowheads mark the first neuronal cells in the mutant patch versus in the surrounding wild-type tissue; note that the arrowhead is two rows closer to the furrow in the wild-type tissue. (F) Eye disc containing a hnt^{XE81} clone visualized by lack of immunostaining with α-HNT antibody (HNT-expressing cells are red). The outlines of emerging R cell clusters are highlighted using α-PY antibody (green). Inside the mutant patch, the arc stage of development looks normal (arrow), but defects in cell arrangement and number can be observed in the preclusters (arrowheads). (G) Eye disc from a wild-type larva stained with the α-Glass antibody, which labels all of the presumptive R cells. Cells of the definitive precluster are labeled with red arrowheads. (H) Eye disc from a hnt^{peb} larva, raised at the restrictive temperature and stained with the α-Glass antibody. Many of the preclusters (yellow arrowheads) have defects, including missing or extra Glass-positive cells and displaced nuclei within a cluster. Red arrowheads point to preclusters with a normal complement of cells.

labels the nuclei of the R3 and R4 precursor cells, beginning two rows posterior to the furrow (Barrio et al., 1999). In *hnt* patches, Boss accumulates in all R8 cells; however, there is a delay of one to two rows relative to the adjacent wild-type tissue and Boss levels are often reduced (Fig. 4A, arrowheads). These results suggest that, although the mutant R8 cell in each precluster is eventually properly determined, the Boss ligand is either not tightly localized to the apical surface of the R8 cell or there are lower amounts of it in the cell.

The rho^{PX81} enhancer trap is expressed within *hnt* patches. However some of the clusters have only one or two nuclei that stain, rather than the predicted three (47%, *n*=129 clusters; Fig. 4B,C). As there are determined R8 cells present in these patches, we hypothesize that the R2 or R5 precursor cells are mis-specified, or fail to be specified, in many of the preclusters and thus do not express the rho^{PX81} enhancer trap. In many clusters (74%), the nuclei are displaced relative to one another (Fig. 4B,C), consistent with a problem in cell shape or cell arrangement within the cluster (as visualized above with the α-PY antibody; Fig. 3F). In 79% of the triads, there are also defects in the rotation of the clusters (Fig. 4B,C).

The α-Spalt antibody, which labels the R3 and R4 precursor cells, also shows aberrant staining within *hnt* patches (Fig. 4D,E). In 57% of clusters, only one cell stains with α-Spalt antibody (*n*=145 clusters). When two nuclei stain, often they are at different planes relative to one another (84% versus 0% in the adjacent wild-type tissue). This result implies that the mutant R3 or R4 precursor cell is mis-shapen or aberrantly positioned in the cluster. In 67% of the clusters the cells fail to rotate correctly.

In summary, our results show that specific furrow markers persist posterior to the furrow in *hnt* mutants, that there is a delay in specification of preclusters as cells exit the furrow, that there are morphological defects in the preclusters, that recruitment of cells into specific R cell fates does not occur and that there are planar polarity defects in *hnt* mutants.

HNT function is required to establish planar polarity in the developing eye

The mutant phenotypes we observed in the developing eye disc suggested that HNT plays a role in establishing planar polarity. To define this role at single cell resolution, we analyzed genetically mosaic ommatidia along the borders of *hnt* mutant

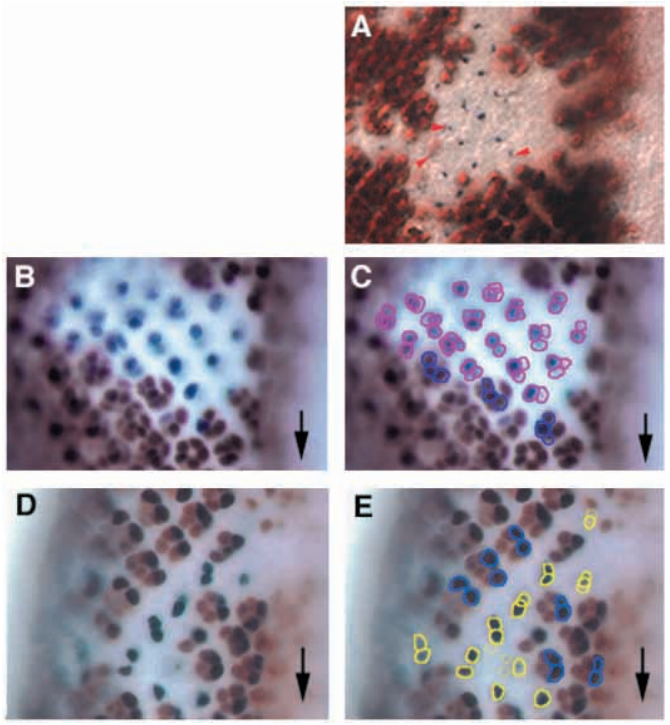

Fig. 4. R-cell specification in preclusters in *hnt* mutants. Eye discs containing clones of *hnt* tissue are shown. In all cases, the clone is marked by a lack of brown α-HNT antibody staining. The location of the furrow together with the direction of the equator is indicated by the arrows. (A) Apical membrane expression of the R8 marker, Boss, visualized by α-Boss antibody immunostaining in blue-black. Within the *hnt* patch, there is always a determined R8 cell, although occasionally there is a lower level of Boss accumulation than normal (red arrowheads). (B,C) Nuclear expression of the rho^{PX81} enhancer trap, which labels determined R8, R2 and R5 precursor cells, visualized by α-β-gal antibody staining in blue-black and outlined in pink in the patch or in blue in surrounding wild-type clusters (C). Within the *hnt* patch, 47% of clusters have one or two non-staining cells, 74% of the clusters have misarrangements of their cells and 79% of the triads show misrotation of the cluster relative to its wild-type counterparts. (D,E) Nuclear expression of Spalt, which labels the R3 and R4 precursor cells, is shown by α-Spalt antibody staining in blue-black. The nuclei of the R3 and R4 cells are outlined in blue in wild-type clusters or in yellow in cells in the *hnt* patch (E). Pale yellow indicates nuclei with reduced α-Spalt staining. Inside the *hnt* patch, 57% of clusters have a non-staining cell, 84% have misarrangements of their cells and 67% show misrotation.

patches in the adult eye. In wild-type ommatidia, each R cell occupies a distinctive position within the trapezoidal array of rhabdomeres (Fig. 5). The *hnt* mosaic ommatidia showed polarity defects, including reversed chirality (56%, *n*=43 defective ommatidia; see Fig. 5A classes II, V and VI), misrotation (44%; see Fig. 5A classes III-VI) and loss of R3/R4 asymmetry (30%; see Fig. 5A classes VII and VIII). The polarity defects within *hnt* patches are restricted to mosaic ommatidia; we did not see any cases where the genetically wild-type ommatidia adjacent to mosaic ommatidia are misoriented. Thus, HNT implements a local function in coordinating polarity establishment within an ommatidium.

By quantifying the genotypes of R cell subtypes in genetically mosaic ommatidia, we determined which R cells required HNT function for establishment of ommatidial polarity. Normal chirality and normal rotation require HNT function in the outer photoreceptor cells (R1-R6), as trapezoidal ommatidia with incorrect chirality and/or rotation always include at least one mutant outer photoreceptor cell (see Fig. 5A classes II-VI and Fig. 5B). Notably, the particular combination of mutant R cells does not predict to what extent an ommatidium will be misrotated or whether it will have reversed chirality. There is, however, a bias in the frequency with which specific R cells are mutant in the misoriented ommatidia (Table 1). For example, cases where the R3 (49%), R4 (36%) or R6 (26%) cells are mutant for *hnt* are somewhat over-represented among defective ommatidia. This finding implies that HNT function may be most important in the R3, R4 and R6 cells for control of ommatidial polarity, although the other outer R cells also clearly make some contribution.

The borders of the hnt^{XE81} and hnt^{XO01} clones also include R3/R3 type symmetrical ommatidia where the R3 or the R4 cell has not taken up the correct position (*n*=12, see Fig. 5A classes VII and VIII and Fig. 5C). In these ommatidia, either the R3 or R4 cells, or both, are mutant for *hnt*, and the chirality, as assayed by the R8 projection, is also sometimes incorrect. These results imply that HNT is required in the R3 and/or R4 cells to establish ommatidial asymmetry. The fact that all of the symmetrical ommatidia are of the R3/R3 type suggests that HNT function is necessary in the R3/R4 pair to determine R4 fate and location; in the absence of HNT, the R4 cell adopts a more R3-like position in the ommatidium.

Given the previously reported role of JNK signaling in establishing planar polarity in the eye (Weber et al., 2000) and the planar polarity defects in *hnt* mutants reported here, we tested for genetic interactions between JNK pathway mutants and hnt^{peb}. Two alleles of *jun* (jun^1, a hypomorph, and jun^2, a genetic null) and two alleles of *basket* (bsk^1 and bsk^2) act as dose-sensitive suppressors of the hnt^{peb} photoreceptor defects, as assayed in histological sections. hnt^{peb}/Y; jun^1/+ eyes show 31% wild-type ommatidia (*n*=775) versus 17% in hnt^{peb}/Y control siblings (*n*=340), and hnt^{peb}/Y; jun^2/+ eyes have 26% wild-type ommatidia (*n*=750) versus 15% in controls (*n*=207). hnt^{peb}/Y; bsk^1/+ eyes show 11% wild-type ommatidia (*n*=828) versus 7% in controls (*n*=509), and hnt^{peb}/Y; bsk^2/+ have 11% wild-type ommatidia (*n*=957) versus 8% in controls (*n*=606). When polarity defects are scored in those ommatidia with wild-type numbers of R cells, from hnt^{peb}/Y; bsk^1/+ eyes, 14% show polarity defects versus 21% in hnt^{peb}/Y controls, whereas in hnt^{peb}/Y; bsk^2/+ eyes, 17% show polarity defects versus 40% in hnt^{peb}/Y controls. The direction of these genetic interactions in the eye is consistent with a role for HNT in downregulating JNK signaling.

In summary, we have shown here that HNT function is required to establish planar polarity in the eye and have presented genetic evidence that this role may be accomplished by downregulation of JNK signaling.

HNT function is required for morphogenesis of the pupal retina and for maintenance of retinal epithelial integrity

In eyes from hnt^{peb} flies raised at the restrictive temperature, the facets in the eye are misaligned, with occasional ommatidial fusions (2.8%) and a small percentage of bristle displacements and bristle size defects (Fig. 2B, Fig. 6A).

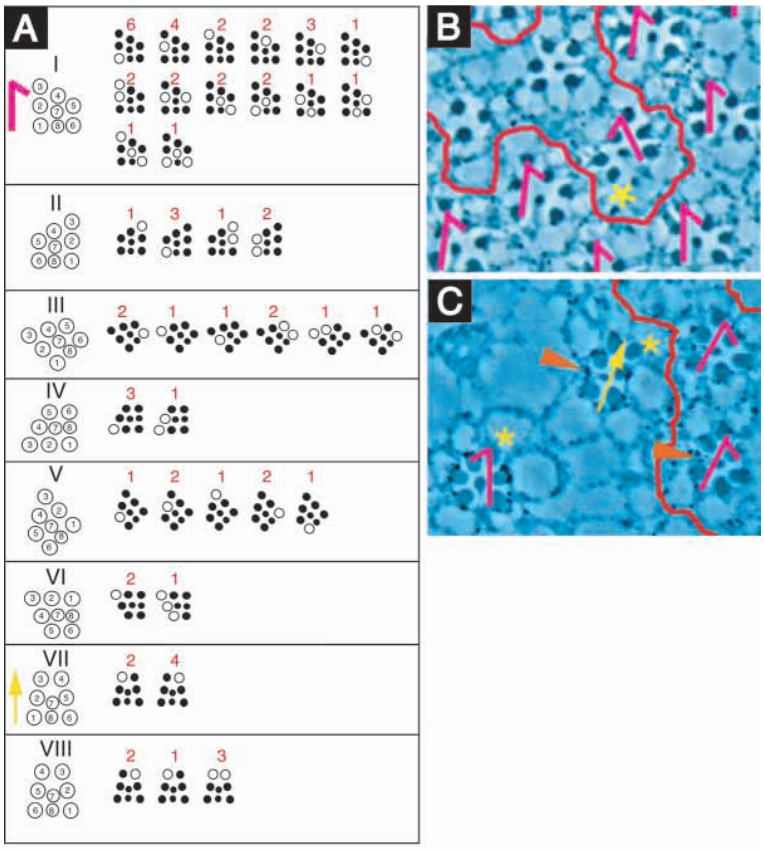

Fig. 5. Mosaic analysis of *hnt* clones in the eye. (A) The results of a clonal analysis of mosaic ommatidia along the borders of 94 *hnt* patches are schematized. Each data set represents ommatidia with different phenotypic organization: I, wild type; II, chiral flip; III, 45°rotation; IV, 90° rotation; V, chiral flip and 45° rotation; VI, chiral flip and 90° rotation; VII, symmetrical; VIII, symmetrical and chiral flip. Black R cells are wild type with respect to *hnt*; white R cells are mutant for *hnt*. The number of ommatidia with that particular phenotype is shown in red. (B) Apical tangential section of a hnt^{XO01} clone (mutant patch is to the left of the red line). The polarity of each ommatidium is labeled with a pink arrow as shown on the schematic in A. The yellow asterisk marks the *hnt* single mutant cell (R6) in a mosaic ommatidium that is an example of class V (i.e. misrotated by 45° and chirally flipped with respect to the adjacent wild-type ommatidia). (C) More basal tangential section of a hnt^{XE81} clone. A class VII symmetrical ommatidium with a mutant R4 cell (asterisk) is labeled with a yellow arrow. The R8 projection (between R1 and R2) is marked with an orange arrowhead. A chirally flipped and misrotated (class V) ommatidium can be seen on the bottom left of the mutant patch. In this case, there is a mutant R3 cell (asterisk).

Table 1. Relative requirements for *hnt* in outer R cells to establish correct polarity

Mutant photoreceptor cell	Misoriented ommatidia*	Wild-type ommatidia†
R1	2	9
R2	2	9
R3	19	5
R4	14	2
R5	6	6
R6	10	5

The outer R cells were scored in ommatidia genetically mosaic for *hnt*.
*The number of examples of misorientated ommatidia that were mutant for the outer R cell.
†How often the R cell was mutant in ommatidia with wild-type orientation.

Transverse sections of eyes from hnt^{peb} flies reveal many photoreceptor cell abnormalities (Fig. 6C versus 6B). Although some ommatidia contain extra apical central cells (Fig. 6C, white arrowhead; 12%, *n*=820 ommatidia), the most common defect is missing photoreceptor cells (Fig. 6C, black arrowheads), including missing outer cells (43%), missing central cells (1%), or missing outer and central R cells (11%).

We determined the temperature-sensitive period of the conditional hnt^{peb} mutant and found that the crucial period for external eye roughness spanned from the mid-third instar to early pupal stages (data not shown). Flies that spent all of this crucial period at the restrictive temperature had the roughest eyes, implying that there is a continuous requirement for HNT function through these stages of development. The fact that flies spending only the early pupal stages at the restrictive temperature [from 2 hour after puparium formation (APF) onwards at 29°C] are also rough-eyed, indicates there is a role for HNT during the differentiation of the retinal epithelium during the pupal period (i.e. after the photoreceptor cells have been patterned and determined). Consistent with this interpretation is the fact that patches of cells homozygous for strong alleles of *hnt* form scars in adult eyes (Fig. 6D). Transverse sections through these scars show that they are devoid of R cells but still contain pigment cells (Fig. 6E). From our studies of *hnt* clones in the larval eye disc, it is clear that this phenotype is not due to a failure of the R cells to develop, but must be a consequence of loss of R cells from the retinal epithelium during the pupal stages. Longitudinal sections through *hnt* clones revealed that ommatidia in which all of the photoreceptor cells are mutant for hnt^{XE81}, hnt^{XO01} or hnt^{EH704a} are unable to maintain their position in the developing epithelium and fall out of the retina onto the lamina of the optic lobe of the brain (Fig. 6F, arrowheads).

To ascertain whether the loss of R cells is a secondary consequence of increased programmed cell death we stained mutant patches for apoptotic cells. *hnt* patches show normal levels of cell death relative to adjacent wild-type eye tissue during late larval stages (data not shown). Thus, cells that are not specified correctly in the preclusters do not die but are reincorporated into the pool of undifferentiated cells in the eye disc. In addition, during early-to-mid pupal stages, there is no increased apoptosis in patches of *hnt* mutant cells relative to adjacent wild-type cells (data not shown; P5, 12.5-25 hour APF and P8, 47-57 hour APF at 25°C, were tested). These results imply that the loss of *hnt* mutant R cells from the retinal epithelium is not a secondary consequence of cell death.

We used the adult eye mosaics described above to ask which R cells require HNT function to maintain the integrity of the retinal epithelium during pupal development. An examination of 94 patches led to the identification of 71 genetically

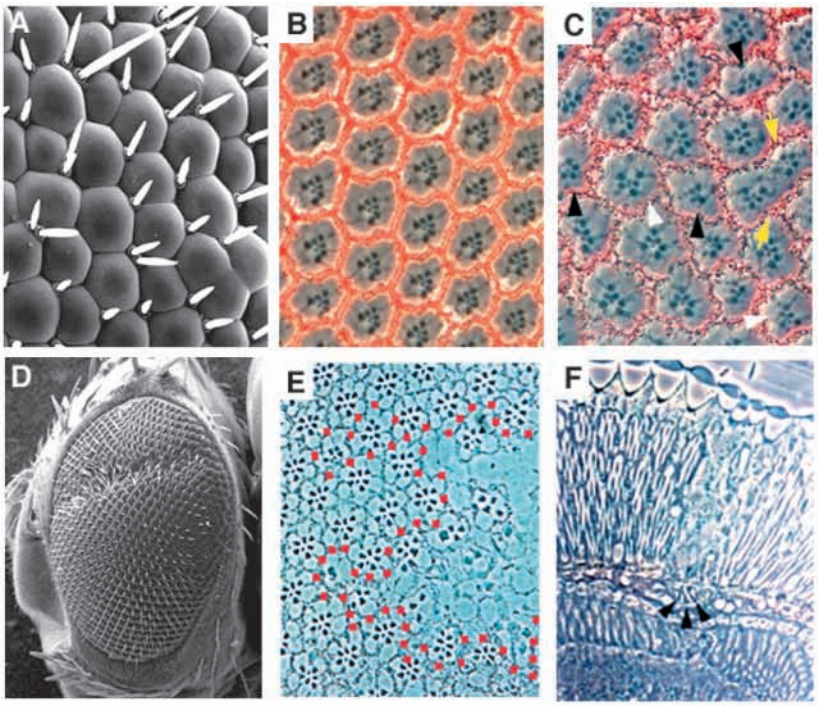

Fig. 6. Adult phenotypes of *hnt* mutants. (A) Scanning electron micrograph (SEM) of part of an eye from a hnt^{peb}/hnt^{peb} fly. Some of the facets do not have the stereotypical hexagonal shape, others are fused. The sensory bristles are sometimes mispositioned and show a variation in size never seen in wild type. (B) Apical tangential section through a wild-type eye, showing each ommatidium with a trapezoidal arrangement of the seven photoreceptor (R) cells. All the ommatidia in this half of the eye have the same polarity. (C) In an eye from a hnt^{peb}/Y fly raised at the restrictive temperature, 40% of the ommatidia are missing outer or central R cells (black arrowheads), 12% have extra R cells (white arrowhead) and some of the ommatidia are fused (yellow arrows point to a pair of fused ommatidia). The ommatidia also have variable polarity. (D) SEM of an eye with a scar caused by a clone of hnt^{XO01} tissue. Clones mutant for three different *hnt* alleles (hnt^{XE81}, hnt^{EH704a} and hnt^{XO01}) form scars. (E) An apical tangential section through a hnt^{XE81} scar (to right of red dots) reveals that the interior of the clone contains no R cells but that pigment cells are still present. (F) A cross section through another hnt^{XE81} scar, shows that some of the R cells (arrowheads) have fallen out of the retinal epithelium. The R cells come to reside on the optic lobe of the brain and the basal, fenestrated membrane of the retina, which is assembled after the R cells fall out of the epithelium (see Fig. 7 and Results), separates these R cells from the retina.

mosaic ommatidia. Typically, in wild-type controls, one medium-sized patch yields about 10 mosaic ommatidia; we would therefore have expected over 900 mosaic ommatidia in our experiment. The more than tenfold under-representation of mixed ommatidia along the borders of *hnt* clones suggests that many of them formed but subsequently lost their integrity. By quantifying the genotypes of R-cell subtypes in surviving mixed-genotype ommatidia, we were able to establish which R cells required HNT function in order for an ommatidium to be wild type with respect to photoreceptor number and internal arrangement (n=59, Fig. 5A classes I-VI). Our analyses show that there must be at least five hnt^{+} R cells – of any subtype – within the ommatidium for maintenance of its integrity in the retinal epithelium.

Beyond its role in maintenance of epithelial integrity, HNT function is also required for normal rhabdomere structure. In a wild-type adult eye, the R1-R6 cell bodies and their rhabdomeres extend over the full apical-to-basal extent of the ommatidial column (schematized in Fig. 7A). In eyes from hnt^{peb} flies some of the photoreceptor cells (4.2%) have enlarged rhabdomeres when viewed in individual histological sections. Such an apparent enlargement could result from failure in apical-to-basal extension of the cell and its rhabdomere. In order to study morphological defects in individual *hnt* mutant adult R cells, we made serial sections through genetically mosaic ommatidia containing cells homozygous for *hnt* alleles. Mutant rhabdomeres fail to extend the normal length of the ommatidial column, indicating that *hnt* cells often have shortened cell bodies (Fig. 7A, left side). This phenotype is R cell autonomous, as all R cells with defective rhabdomeres are also mutant for *hnt*. During the late pupal period (110 hour APF), the rhabdomeres of the individual R cells within an ommatidium separate from each other to give the canonical trapezoidal pattern found in the adult (Cagan and Ready, 1989a). An additional defect found in serial sections of *hnt* genetic mosaic ommatidia is failure of rhabdomere separation (Fig. 7A, right side): rhabdomere separation is often normal in the apical region of the ommatidium but, as one proceeds basally, one can observe failure of the rhadomere of a *hnt* mutant cell to separate from its wild-type neighbor (Fig. 7A, right side).

To investigate the developmental basis for the morphological defects in individual R cells, as well as the loss of R cells from the retinal epithelium, we stained larval and pupal discs with phalloidin-FITC, which binds to and labels the polymerized form of actin (filamentous actin or F-actin). F-actin is concentrated at the apical tip of the cells in preclusters in wild-type larval discs (Fig. 7B). Later, F-actin is present in the elongating rhabdomeres in pupal discs (Figs. 7C,D) (Longley and Ready, 1995; Sang and Ready, 2002). When patches of hnt^{XE81}, hnt^{EH704a} or hnt^{XO01} cells in larval discs are stained with phalloidin, the F-actin localization is depleted and/or more diffusely localized, particularly in the more posterior regions of the mutant part of the disc (Fig. 7B). This disruption of F-actin distribution is probably not due to a late change in the apical constriction of clusters as α-PY antibody-stained discs look fairly normal with respect to these more posterior clusters (see Fig. 3F). Depletion of apical F-actin is also evident in *hnt* patches in early pupal discs (stage P5; data not shown). By later pupal stages (P8/9, 47-69 APF at 25°C) the R cells from ommatidia that lack all *hnt* function have dropped out of the epithelium (Fig. 7C,D). Ommatidia mosaic for *hnt* function have a lower concentration of F-actin in their R cells and it is found more basally than in their wild-type neighbors (arrows, Fig. 7C,D). This defect in actin polymerization or assembly may be a developmental precursor to the rhabdomere phenotype observed for mutant photoreceptor cells in the adult eye (Fig. 7A).

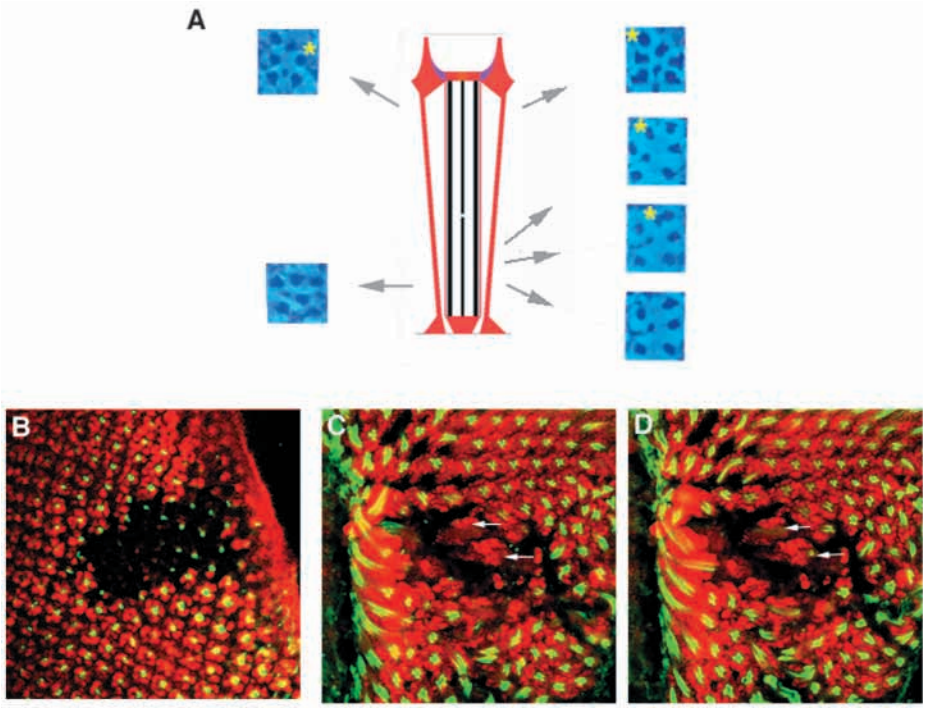

Fig. 7. Rhabdomere structure and integrity in *hnt* mutants. (A) Schematic of a longitudinal section through an adult ommatidium, showing the rhabdomeres (black) extending along the apicobasal axis of the eye epithelium. Gray arrows indicate the level of transverse cross-sections through two distinct mosaic ommatidia, shown in the blue panels either side of the schematic. The mosaic ommatidium on the left has an R5 cell that is mutant for *hnt*. The R5 rhabdomere is seen in an apical plane of section (yellow asterisk), but does not extend all the way basally, unlike the rhabdomeres belonging to the other, hnt^{+}, outer R cells in this ommatidium. The mosaic ommatidium on the right has an R3 cell that is mutant for *hnt* (yellow asterisk). At an apical plane of section the rhabdomeres have a wild-type appearance, whereas, at more basal levels, the R3 and R4 rhabdomeres have failed to separate. (B) Third instar larval eye disc stained with an α-HNT antibody (red), which is absent from the hnt^{XO01} patch, and phalloidin-FITC (green), which stains the F-actin concentrated at the apical tips of the developing photoreceptor cell clusters. The F-actin is depleted in the more posterior area of the *hnt* patch compared with its levels in the adjacent wild-type tissue. (C) Apical section of a late pupal disc stained with α-HNT antibody (red) and phalloidin-FITC (green), and containing a clone of hnt^{XE81} tissue. In the area where the R cells are all mutant, there is no F-actin accumulation. HNT-positive R cells within two mosaic ommatidia along the clone border (arrows) have less F-actin apically than their genetically wild-type neighbors within the cluster. (D) More basal view of the same clone as in C, showing that there are low levels of F-actin in the more basal regions of these cells (arrows).

DISCUSSION

Morphology and determination of individual cells and cell clusters

The earliest defects we observed in *hnt* mutant eye tissue occur during the formation of the definitive five-cell ommatidial preclusters. Specifically, we have shown that there is a 4 hour delay in specification of the ommatidial preclusters relative to wild type, the shape of individual R cells within these preclusters is often abnormal, and the relative orientation of the presumptive R cells within a precluster is disrupted. There are two plausible explanations for the observed defects: a failure in cell cycle synchronization or abnormal cellular morphology. First, it has been shown that lack of cell cycle synchronization in the furrow can lead to a one to two column delay in R cell precursor determination (e.g. in *roughex* mutants) (Thomas et al., 1994). Furthermore, a precluster phenotype in which nuclei are inappropriately positioned in the apicobasal plane relative to one another, is seen in mutants disrupted for cell cycle synchronization in the furrow (e.g. *thick vein*, *saxophone*, *schnurri*) (Penton et al., 1997). Thus, it is possible that failure of cell cycle synchronization underlies the *hnt* mutant phenotypes described here. Alternatively, the primary defect in *hnt* mutants might be the abnormal morphology of the R cells. For example, the *act up* mutant, which alters the apical morphology of the precluster cells, shows premature *dpp* expression, premature R cell differentiation and uncoordinated neuronal determination (Benlali et al., 2000). We have shown here that *dpp* expression persists posterior to the furrow in eye discs of hypomorphic *hnt* mutants. This phenotype is distinct from that described for *act up* or, to our knowledge, any other mutant. It is consistent, however, with our previous analyses demonstrating a role for HNT in downregulation of *dpp* expression in the amnioserosa (Reed et al., 2001).

Planar polarity

Our results obtained from mosaic analysis of *hnt* alleles clearly demonstrate that HNT function is necessary in all of the outer R cells in the developing eye disc, particularly in the R3, R4 and R6 precursor cells, for correct planar polarity. A role for the R3 and R4 precursor cells in establishing planar polarity in the eye has previously been proposed on the basis of analyses of the JNK pathway in this process (Weber et al., 2000). Those experiments could not rule out a role for other outer R precursor cells, which also express the JUN transcription factor (Bohmann et al., 1994; Weber et al., 2000). *hindsight* must now be added to the list of genes, such as *strabismus* (Wolff and Rubin, 1998), that regulate planar polarity and have a clearly described role in all of the outer R cells.

The fact that all of the symmetrical ommatidia along the borders of *hnt* clones are of the R3/R3 conformation suggests that HNT function is necessary for correct R4 fate and orientation. It has been suggested that, owing to its closer proximity to the polarizing signal from the equator, a stronger activation of the JNK pathway occurs in the R3 precursor cell (Weber et al., 2000). Activated JUN would then be responsible for the upregulation of the target gene, *Delta*, in the R3 precursor cell relative to the R4 precursor cell (Weber et al.,

2000). As our results in the eye (this study) and results in the embryo (Reed et al., 2001) imply that HNT is necessary for downregulating JNK function, we propose that the wild-type function of HNT is to downregulate JNK activity in the R4 precursor cell. Such downregulation would enhance JNK signaling differences between the R3 and R4 cells. In the absence of the HNT gene product, JNK signaling would be inappropriately elevated in the R4 precursor cell, thereby upregulating the transcription of JNK targets such as *Delta*, leading that cell to behave more like a R3 precursor cell. Consistent with this model, we have found that *Delta* hypomorphs act as enhancers of the hnt^{peb} rough eye phenotype (A. T. P., R. Wilk and H. D. L., unpublished). R3/R3 symmetric clusters are observed both when the R4 cell is mutant for *hnt* and the R3 precursor is hnt^{+}, and when the R3 cell is mutant for *hnt* and the R4 precursor is hnt^{+}. In the latter case, the above model would lead one to expect normal R3/R4 clusters. As only R3/R3 clusters are observed, we speculate that HNT can affect the R4 precursor cell when expressed only in the neighboring R3 precursor cell (i.e. that there may be some communication feedback between these cells leading to local non-autonomy of the *hnt* phenotype).

The early morphological and fate determination defects and the later planar polarity defects seen in *hnt* eyes may be causally connected. We have shown that specification of the early outer R cell precursors (R2, R5, R3 and R4) is often disrupted in *hnt* tissue. It has been established that early disruption of R3 and R4 fate can perturb planar polarity (e.g. in the *seven-up* mutant) (Fanto et al., 1998). This result suggests that accurate interpretation of extrinsic polarity signals may require each R cell to already be properly determined. We have also shown that the relative positioning of outer R cells within a precluster is frequently deviant in *hnt* mutants before precluster rotation. Therefore the relative distance to the equator, or to a neighboring cluster, may also be crucial for differential reading of the polarity signal by pairs of outer cells within the cluster (R3 versus R4, R2 versus R5).

The F-actin-based cytoskeleton

Our previous analyses have shown that that HNT function in the amnioserosa is required for the assembly and/or maintenance of focal complexes in adjacent epithelial cells along the leading edge of the dorsal ectoderm (Reed et al., 2001). We have demonstrated that these F-actin rich structures, which also accumulate high levels of α-PY reactive proteins, are required for morphogenetic events during normal dorsal closure. In wild-type eye discs, F-actin is enriched at the apical tips of presumptive R cells in ommatidial preclusters. This apical F-actin forms part of a tightly localized signaling complex enriched for receptor and ligand molecules such as Sevenless (Banerjee et al., 1987; Tomlinson et al., 1987), Boss (Van Vactor et al., 1991), Notch (Fehon et al., 1991) and Delta (Kooh et al., 1993). Here, we have shown that, in late larval eye discs, *hnt* mutant R cells have reduced F-actin at their apical tips. Furthermore, although the R8 precursor cell is correctly determined in *hnt* mutant patches, the Boss ligand is less concentrated at the apical tips of some of the *hnt* R8 cells. The F-actin phenotype seen in *hnt* patches in larval eye discs occurs late and is therefore probably not a direct cause of disruption of the apical signaling complex in the eye disc. However, the defects in F-actin accumulation may be a marker indicative of perturbed cytoarchitecture in the apical region of the mutant R cell. Such a perturbation would have serious consequences for correct R cell specification, which requires intimate contacts between adjacent R cells for proper intercellular signaling.

We have shown that, in the pupal retina, the concentration of F-actin in the apical tips of the R cell clusters is depleted in *hnt* mutant eye tissue. Still later, less F-actin accumulates in the extended rhabdomeres. F-actin and associated proteins in the apical surfaces of the photoreceptors play a key role in the initiation of rhabdomere morphogenesis (Cagan and Ready, 1989a; Longley and Ready, 1995; Sang and Ready, 2002). In addition, F actin is a component of the rhabdomere terminal web, a structure that anchors the rhabdomere membranes along the length of the differentiating R cell and prevents them from collapsing into the R-cell cytoplasm (Chang and Ready, 2000). When the function of Drac1, which regulates F-actin arrangement, is disrupted, the rhabdomere membranes ‘spool out’ into the cytoplasm (Chang and Ready, 2000). Interestingly, in addition to its role in rhabdomere morphogenesis, Drac1 is thought to signal through the JNK cascade and, like HNT, is necessary earlier on for the establishment of planar polarity in the eye (Fanto et al., 2000) and for dorsal closure of the embryo (Harden et al., 1995; Harden et al., 1999; Reed et al., 2001). The pupal photoreceptor phenotype that we observe in *hnt* R cells, where rhabdomeres do not extend fully in the apicobasal axis, is qualitatively different from that seen for a dominant negative Drac1 allele (Chang and Ready, 2000).

We speculate that the depletion of F-actin in *hnt* mutant R cells may affect morphogenetic events that precede rhabdomere terminal web maturation. For example, there may be defects in extension of the specialized membrane down the length of the R cell or in closure of cone cells over the highly constricted R cell apices (Cagan and Ready, 1989a; Longley and Ready, 1995; Sang and Ready, 2002). The morphogenetic parallels between closure of the leading edge epidermal cells over the constricted amnioserosa of the embryo and closure of the cone cells over the constricted R cell apices in the pupal eye are striking. Furthermore, both require assembly and function of F-actin-rich complexes at the boundary between the two cell types involved.

Maintenance of epithelial integrity

We have shown that *hnt* mutant R cells are unable to maintain their integrity within the retinal epithelium during retinal differentiation and morphogenesis in pupal discs. By analogy, the *hnt* phenotype in the tracheal system is first seen at stage 14, when the overtly normal tracheal epithelium begins to disintegrate, forming sacs and vesicles from the collapsed dorsal trunk and branches (Wilk et al., 2000). In *hnt* hypomorphs, a specific proportion of the cells in the amnioserosa fall out of the epithelium during dorsal closure (B. A. Reed and H. D. L., unpublished). Thus, HNT function is required for maintenance of the integrity of the epithelia in which it is expressed.

In the eye, loss of integrity occurs in clusters containing fewer than five out of eight HNT-expressing R cells. We speculate that delamination of clusters may occur because they lack a threshold level of apical F-actin required for inter-photoreceptor communication and/or adhesion. For example, if *hnt* mutant R cells fail to form focal contacts with the

overlying cone cells, a genetically mosaic R cell cluster could slip basally, eventually falling out of the epithelium before consolidation of the fenestrated membrane during the pupal period.

In the eye, patches of tissue mutant for certain of the integrins (*myospheroid* and *inflated*) have missing R cells or R cells with shortened rhabdomeres (Zusman et al., 1993; Zusman et al., 1990). Detailed studies have shown that integrins are expressed in the cone and pigment cells and that the mutant phenotypes may trace their origin to a structural defect in the cone cell plate at the retinal floor (Longley and Ready, 1995). HNT is not expressed in cone or pigment cells and there is no gross defect in the retinal floor beneath *hnt* mutant eye tissue. However, as we observe an F-actin defect and it is known that extracellular engagement of adhesion molecules physically links F-actin bundles with the cell surface to provide structural integrity, further studies to examine possible requirements of HNT for extracellular matrix production or function may be revealing.

Conclusions

Our results clearly implicate HNT in regulation of several types of cellular events that are common to the different contexts in which it functions. These include establishment or maintenance of the morphology of individual cells within an epithelium, as well as maintenance of the integrity of the epithelium per se (this study) (Lamka and Lipshitz, 1999; Reed et al., 2001; Wilk et al., 2000). There are also shared molecular correlates of these HNT functions. In particular, HNT is required for establishment of localized F-actin- and phosphotyrosine-rich complexes in the leading edge epidermal cells, as well as in the photoreceptor cells (this study) (Reed et al., 2001). We have also presented evidence that HNT functions to regulate two JNK signaling dependent processes, planar polarity in the eye and dorsal closure of the embryo (this study) (Reed et al., 2001), possibly by downregulating JNK signaling in time and space. Whether the functions of HNT in different tissues and at different times during development derive from control of the same molecular pathway will await genetic and molecular analysis of the genes regulated by HNT.

We thank an anonymous reviewer for insightful comments on the parallels between closure of embryonic epidermal leading edge cells over the amnioserosa and cone cell closure over the R cells during retinal morphogenesis; these have been integrated into the Discussion. We also thank Dr D. Ready for helpful advice and discussions upon our initiation of this research project; Drs S. L. Zipursky, K. Moses and R. Barrio for supplying antibodies; Dr M. Mlodzik and the Bloomington *Drosophila* Stock Centre for providing fly stocks. We are grateful to Drs J. Brill, T. Erclik, R. McInnes, B. Reed, K. Yee and R. Wilk for helpful comments on the manuscript. A. T. P. was supported in part by a postdoctoral fellowship from the Research Training Center of the Hospital for Sick Children, M. L. L. by a postdoctoral National Research Service Award from the USPHS and M. L. R. Y. in part by a predoctoral fellowship from the Howard Hughes Medical Institute. This work was funded by a an operating grant to H. D. L. from the National Cancer Institute of Canada with funds from the Canadian Cancer Society.

REFERENCES

Banerjee, U., Renfranz, P. J., Hinton, D. R., Rabin, B. A. and Benzer, S. (1987). The sevenless+ protein is expressed apically in cell membranes of developing Drosophila retina; it is not restricted to cell R7. *Cell* **51**, 151-158.

Barrio, R., de Celis, J. F., Bolshakov, S. and Kafatos, F. C. (1999). Identification of regulatory regions driving the expression of the Drosophila spalt complex at different developmental stages. *Dev. Biol.* **215**, 33-47.

Benlali, A., Draskovic, I., Hazelett, D. J. and Treisman, J. E. (2000). act up controls actin polymerization to alter cell shape and restrict Hedgehog signaling in the Drosophila eye disc. *Cell* **101**, 271-281.

Blackman, R. K., Sanicola, M., Raftery, L. A., Gillevet, T. and Gelbart, W. M. (1991). An extensive 3′ cis-regulatory region directs the imaginal disk expression of decapentaplegic, a member of the TGF-beta family in Drosophila. *Development* **111**, 657-666.

Bohmann, D., Ellis, M. C., Staszewski, L. M. and Mlodzik, M. (1994). Drosophila Jun mediates ras-dependent photoreceptor determination. *Cell* **78**, 973-986.

Boulianne, G. L., de la Concha, A., Campos-Ortega, J. A., Jan, L. Y. and Jan, Y. N. (1991). The Drosophila neurogenic gene neuralized encodes a novel protein and is expressed in precursors of larval and adult neurons. *EMBO J.* **10**, 2975-2983.

Cagan, R. L. and Ready, D. F. (1989a). The emergence of order in the Drosophila pupal retina. *Dev. Biol.* **136**, 346-362.

Cagan, R. L. and Ready, D. F. (1989b). Notch is required for successive cell decisions in the developing Drosophila retina. *Genes Dev.* **3**, 1099-1112.

Chang, H.-Y. and Ready, D. F. (2000). Rescue of photoreceptor degeneration in rhodopsin-null Drosophila mutants by activated Rac1. *Science* **290**, 1978-1980.

Fanto, M., Mayes, C. A. and Mlodzik, M. (1998). Linking cell-fate specification to planar polarity: determination of the R3/R4 photoreceptors is a prerequisite for the interpretation of the Frizzled mediated polarity signal. *Mech. Dev.* **74**, 51-58.

Fanto, M., Weber, U., Strutt, D. I. and Mlodzik, M. (2000). Nuclear signaling by Rac and Rho GTPases is required in the establishment of epithelial planar polarity in the Drosophila eye. *Curr. Biol.* **10**, 979-988.

Fehon, R. G., Johansen, K., Rebay, I. and Artavanis-Tsakonas, S. (1991). Complex cellular and subcellular regulation of Notch expression during embryonic and imaginal development of Drosophila: implications for Notch function. *J. Cell Biol.* **113**, 657-669.

Freeman, M., Kimmel, B. E. and Rubin, G. M. (1992). Identifying targets of the rough homeobox gene of Drosophila: evidence that rhomboid functions in eye development. *Development* **116**, 335-346.

Golic, K. G. (1991). Site-specific recombination between homologous chromosomes in Drosophila. *Science* **252**, 958-961.

Harden, N., Loh, H. Y., Chia, W. and Lim, L. (1995). A dominant inhibitory version of the small GTP-binding protein Rac disrupts cytoskeletal structures and inhibits developmental cell shape changes in Drosophila. *Development* **121**, 903-914.

Harden, N., Ricos, M., Ong, Y. M., Chia, W. and Lim, L. (1999). Participation of small GTPases in dorsal closure of the Drosophila embryo: distinct roles for Rho subfamily proteins in epithelial morphogenesis. *J. Cell Sci.* **112**, 273-284.

Harrison, D. A. and Perrimon, N. A. (1993). Simple and efficient generation of marked clones in Drosophila. *Curr. Biol.* **13**, 424-433.

Hou, X. S., Goldstein, E. S. and Perrimon, N. (1997). Drosophila Jun relays the Jun amino-terminal kinase signal transduction pathway to the Decapentaplegic signal transduction pathway in regulating epithelial cell sheet movement. *Genes Dev.* **11**, 1728-1737.

Huang, F., Dambly-Chaudiere, C. and Ghysen, A. (1991). The emergence of sense organs in the wing disc of Drosophila. *Development* **111**, 1087-1095.

Kiehart, D. P., Galbraith, C. G., Edwards, K. A., Rickol, W. L. and Montague, R. A. (2000). Multiple forces contribute to cell sheet morphogenesis for dorsal closure in Drosophila. *J. Cell Biol.* **149**, 471-490.

Kockel, L., Zeitlinger, J., Staszewski, L. M., Mlodzik, M. and Bohmann, D. (1997). Jun in Drosophila development: redundant and nonredundant functions and regulation by two MAPK signal transduction pathways. *Genes Dev.* **11**, 1748-1758.

Kooh, P. J., Fehon, R. G. and Muskavitch, M. A. (1993). Implications of dynamic patterns of Delta and Notch expression for cellular interactions during Drosophila development. *Development* **117**, 493-507.

Lamka, M. L. and Lipshitz, H. D. (1999). Role of the amnioserosa in germ band retraction of the Drosophila melanogaster embryo. *Dev. Biol.* **214**, 102-12.

Longley, R. L., Jr and Ready, D. F. (1995). Integrins and the development of three-dimensional structure in the Drosophila compound eye. *Dev. Biol.* **171**, 415-433.

Mlodzik, M. (1999). Planar polarity in the Drosophila eye: a multifaceted view of signaling specificity and cross-talk. *EMBO J.* **18**, 6873-6879.

Moses, K. and Rubin, G. M. (1991). Glass encodes a site-specific DNA-binding protein that is regulated in response to positional signals in the developing Drosophila eye. *Genes Dev.* **5**, 583-593.

Penton, A., Selleck, S. B. and Hoffmann, F. M. (1997). Regulation of cell cycle synchronization by decapentaplegic during Drosophila eye development. *Science* **275**, 203-206.

Ready, D. F., Hanson, T. E. and Benzer, S. (1976). Development of the Drosophila retina, a neurocrystalline lattice. *Dev. Biol.* **53**, 217-240.

Reed, B. H., Wilk, R. and Lipshitz, H. D. (2001). Downregulation of Jun kinase signaling in the amnioserosa is essential for dorsal closure of the Drosophila embryo. *Curr. Biol.* **11**, 1098-1108.

Sang, T.-K. and Ready, D. F. (2002). Eyes closed, a Drosophila p47 homolog, is essential for photoreceptor morphogenesis. *Development* **129**, 143-145.

Shellenbarger, D. L. and Mohler, J. D. (1975). Temperature-sensitive mutations of the Notch locus in Drosophila melanogaster. *Genetics* **81**, 143-162.

Sluss, H., Han, Z., Barrett, T., Davis, R. J. and Ip, Y. T. (1996). A JNK signal transduction pathway that mediates morphogenesis and an immune response in Drosophila. *Genes Dev.* **10**, 2745-2758.

Thomas, B. J., Gunning, D. A., Cho, J. and Zipursky, S. L. (1994). Cell cycle progression in the developing Drosophila eye: roughex encodes a novel protein required for the establishment of G1. *Cell* **77**, 1003-1014.

Tomlinson, A. (1985). The cellular dynamics of pattern formation in the eye of Drosophila. *J. Embryol. Exp. Morphol.* **89**, 313-331.

Tomlinson, A., Bowtell, D. D. L., Hafen, E. and Rubin, G. M. (1987). Localization of the sevenless protein, a putative receptor for positional information, in the eye imaginal disc of Drosophila. *Cell* **51**, 143-150.

Tomlinson, T. and Ready, D. (1987). Neuronal differentiation in the Drosophila ommatidium. *Dev. Biol.* **120**, 366-376.

Van Vactor, D. L., Jr, Cagan, R. L., Krämer, H. and Zipursky, S. L. (1991). Induction in the developing compound eye of Drosophila: multiple mechanisms restrict R7 induction to a single retinal precursor cell. *Cell* **67**, 1145-1155.

Weber, U., Paricio, N. and Mlodzik, M. (2000). Jun mediates Frizzled-induced R3/R4 cell fate distinction and planar polarity determination in the Drosophila eye. *Development* **127**, 3619-3629.

Wilk, R., Reed, B. H., Tepass, U. and Lipshitz, H. D. (2000). The hindsight gene is required for epithelial maintenance and differentiation of the tracheal system in Drosophila. *Dev. Biol.* **219**, 183-196.

Wolff, T. (2000). Histological techniques for the Drosophila eye. Part 1: Larva and pupa. In *Drosophila Protocols* (ed. W. Sullivan M. Ashburner and R. S. Hawley), pp. 201-227. Cold Spring Harbor: Cold Spring Harbor Laboratory Press.

Wolff, T. and Ready, D. F. (1991). The beginning of pattern formation in the Drosophila compound eye: the morphogenetic furrow and the second mitotic wave. *Development* **113**, 841-850.

Wolff, T. and Ready, D. F. (1993). Pattern formation in the Drosophila retina. In *The Development of* Drosophila melanogaster, Vol. 2, pp. 1277-1325. Cold Spring Harbor: Cold Spring Harbor Laboratory Press.

Wolff, T. and Rubin, G. M. (1998). Strabismus, a novel gene that regulates tissue polarity and cell fate decisions in Drosophila. *Development* **125**, 1149-1159.

Xu, T. and Rubin, G. M. (1993). Analysis of genetic mosaics in developing and adult Drosophila tissues. *Development* **117**, 1223-1237.

Yip, M. L. R., Lamka, M. L. and Lipshitz, H. D. (1997). Control of germ-band retraction in Drosophila by the zinc-finger protein HINDSIGHT. *Development* **124**, 2129-2141.

Zusman, S., Patel-King, R. S., Ffrench-Constant, C. and Hynes, R. O. (1990). Requirements for integrins during Drosophila development. *Development* **108**, 391-402.

Zusman, S., Grinblat, Y., Yee, G., Kafatos, F. C. and Hynes, R. O. (1993). Analyses of PS integrin functions during Drosophila development. *Development* **118**, 737-750.